ENVIRONMENTAL RESEARCH
LETTERS

LETTER • OPEN ACCESS

Surface impacts of large offshore wind farms

To cite this article: Maryam Golbazi *et al* 2022 *Environ. Res. Lett.* **17** 064021

ENVIRONMENTAL RESEARCH
LETTERS

LETTER

Surface impacts of large offshore wind farms

Maryam Golbazi[1], Cristina L Archer[1,*] and Stefano Alessandrini[2]

[1] Center for Research in Wind (CReW), University of Delaware, 221 Academy Street, Newark, DE, 19716, United States of America
[2] National Center for Atmospheric Research, 3450 Mitchell LnMitchell Ln, Boulder, CO, 80301, United States of America
* Author to whom any correspondence should be addressed.

E-mail: carcher@udel.edu

Keywords: offshore wind, surface temperature, wind turbine, wind farm impacts, wind energy

Supplementary material for this article is available online

OPEN ACCESS

RECEIVED
25 February 2022

REVISED
27 April 2022

ACCEPTED FOR PUBLICATION
10 May 2022

PUBLISHED
25 May 2022

Abstract

Future offshore wind farms around the world will be built with wind turbines of size and capacity never seen before (with diameter and hub height exceeding 150 and 100 m, respectively, and rated power exceeding 10 MW). Their potential impacts at the surface have not yet been studied. Here we conduct high-resolution numerical simulations using a mesoscale model with a wind farm parameterization and compare scenarios with and without offshore wind farms equipped with these 'extreme-scale' wind turbines. Wind speed, turbulence, friction velocity, and sensible heat fluxes are slightly reduced at the surface, like with conventional wind turbines. But, while the warming found below the rotor in stable atmospheric conditions extends to the surface with conventional wind turbines, with extreme-scale ones it does not reach the surface, where instead minimal cooling is found. Overall, the surface meteorological impacts of large offshore wind farms equipped with extreme-scale turbines are statistically significant but negligible in magnitude.

1. Introduction and background

Wind energy is undeniably beneficial to humanity because wind farms replace fossil fuel power plants and their associated air pollution and greenhouse gas emissions while generating clean, renewable, and inexhaustible electricity. However, building large wind farms in the ocean might alter the atmospheric conditions near the surface not only offshore, but also onshore at highly-populated coastal areas. The hypothesis proposed and addressed here is that, as future offshore wind farms will be built with wind turbines of extraordinary size in terms of installed capacity (greater than 10 MW) and dimensions (diameter and hub height greater than 150 and 100 m, respectively), referred to as 'extreme-scale' wind turbines, the surface impacts may differ from those of conventional turbines that have been studied in the literature.

Wind turbines extract kinetic energy from the atmosphere. As a result, wakes are formed, which are plume-like volumes downwind of the wind turbines characterized by lower wind speed and higher turbulent kinetic energy (TKE) compared to the undisturbed wind upstream [6, 45]. Studies have shown that the wakes produced by wind farms can reduce the wind speed by 2–2.5 m s^{-1} [2, 49] and can travel over 20 km [34, 49], in some cases extending to 40–50 km [2, 17] and up to 70 km [21], depending on factors like atmospheric stability or topography [49]. This suggests that the wakes of offshore wind farms might impact surface temperature and other atmospheric properties not only offshore, but potentially also onshore along the coast if the wakes are long enough to reach the land.

There are many studies in the scientific literature about the impacts on near-surface temperature caused by onshore wind farms of different scales (using turbines with 70–100 m hub height varying between 1.5 and 5 MW in capacity) in the U.S. [9, 16, 20, 38, 53, 54], Europe [14], and China [48, 49], but only a few have focused on offshore wind farms [18, 34] and none on extreme-scale offshore wind turbines. The average height and rotor diameter of the turbines used in the literature are approximately 84 and 90 m, respectively. Future wind turbines will be significantly larger and yet, there are no studies in the literature that investigate the impacts of

the turbine size on surface properties by considering extreme-scale turbines and comparing them to conventional turbines. In addition, there are no studies yet that analyze the impacts of offshore wind farms as large as the planned U.S. offshore wind energy areas (WEAs). This study fills these two gaps in the literature by providing an analysis of the sensitivity of surface impacts to turbine hub height, as well as the cumulative impacts of the large U.S. WEAs, including their potential impacts on coastal areas.

Onshore conventional wind turbines have been documented to cause warming at the surface during stable atmospheric conditions [7, 9, 14, 16, 20, 38, 50, 51, 54]. In stable conditions, vertical motion is suppressed and the lapse rate is sub-adiabatic; in unstable conditions, vertical motion is enhanced and the lapse rate is super-adiabatic; and in neutral conditions, vertical motion is neither suppressed nor enhanced and the lapse rate is adiabatic. Onshore, stable conditions are common in winter [40] or at night time [22], but offshore they are more common in summer, regardless of day or night. At first, the accepted mechanism to explain the temperature changes was that the high turbulence in the wakes would reach the ground and cause enhanced vertical mixing, leading to warming and cooling near the surface in stable and unstable conditions, respectively [9, 16, 31, 54]. Recently, however, the enhanced vertical mixing hypothesis has been found untrue. In the onshore VERTEX field campaign [7, 50], by comparing TKE, momentum, and heat fluxes near the ground with and without a wind turbine wake, no evidence of enhanced vertical mixing was found near the ground, despite observed changes in near-surface temperature. Large offshore wind farms in the North Sea have also been found to cause a reduction in sensible heat flux [13], confirming the lack of enhanced vertical mixing near the surface offshore, accompanied by cooling in the summer within the wind farm areas and further downstream.

Given that temperature changes induced by wind farms appear to be strongest during stable atmospheric conditions and that stable conditions are dominant during the summer in the marine environment [5], we base our study on summer of 2018.

It is a challenging task to directly measure the impacts of wind farms on the local environment, even more so offshore, because of the multi-scale nature of the turbulence from the turbines, the dynamic nature of the wakes, and the relatively large horizontal and vertical extents. On the other hand, resolving explicitly every eddy that may form around every individual wind turbine in a wind farm is an almost impossible task due to the excessively high computational demand of such simulations. Thus, to leverage the power of sophisticated simulations without excessive computational requirements, we must use a parameterization approach, which is a simplified treatment that considers the spatially-aggregated impact of wind turbines on the resolved variables. A wind farm is parameterized as an elevated sink of momentum and kinetic energy and an elevated source of TKE. This approach was initially introduced by Baidya *et al* [9], followed by the work by Blahak *et al* [12], and improved by Fitch *et al* [16, 17], which is now implemented in the weather research and forecasting (WRF) model [36, 37] used in this study. Although a few alternatives and improvements to the Fitch parameterization have been proposed [1, 8, 28, 46], here we use it because it performs best at the resolution and with the settings chosen for this study [15]. To use the wind farm parameterization, it is necessary to provide information on wind turbine properties, such as size, rated power, and efficiency. In this study, we use the DTU-10MW offshore wind turbine [10]. The DTU-10MW wind turbine is an example of extreme-scale offshore wind technology that will be used in the next decade in offshore wind projects. Future offshore wind turbines may exceed this size and capacity, but it is unlikely that they will be smaller. We also utilize the Gamesa G128-4.5MW as an example of conventional turbine and the NREL-15MW turbine as another example of an extreme-scale turbine for a sensitivity analysis.

2. Methods

Since the next-generation extreme-scale wind turbines are yet to be deployed, we adopt a modeling approach to study their potential impacts in the offshore environment. We select the Advanced Research WRF modeling system, version 4.3 [37], one of the most widely used numerical weather prediction models. An advantage of the WRF model is that it comes already equipped with the Fitch wind farm parameterization [16, 17]. In this parameterization, the wind turbines are treated as a sink of kinetic energy and a source of TKE. The power extracted from the flow and the power generated by the turbines are calculated as a function of hub-height wind speed using the thrust coefficient (C_T) and the power coefficient (C_P), respectively, which are two important aerodynamic parameters that are turbine-specific. Since information on the C_T and C_P of new turbines is proprietary or difficult to obtain from the manufacturers, here we use the reference DTU-10MW wind turbine [10], which, at the time of this study, is the largest turbine with publicly available aerodynamic information. The diameter D is 178 m, the hub height H is 119 m, and the rated capacity is DTU-10MW (table 1). To assess the sensitivity of the results to the turbine hub height, we also use a second smaller wind turbine, the Gamesa G128-4.5MW turbine ($D = 128$ m and $H = 81$ m) with lower rated capacity (4.5 MW), and a third even taller extreme-scale turbine, the NREL-15 MW turbine ($D = 240$ m and $H = 150$ m) (table 1).

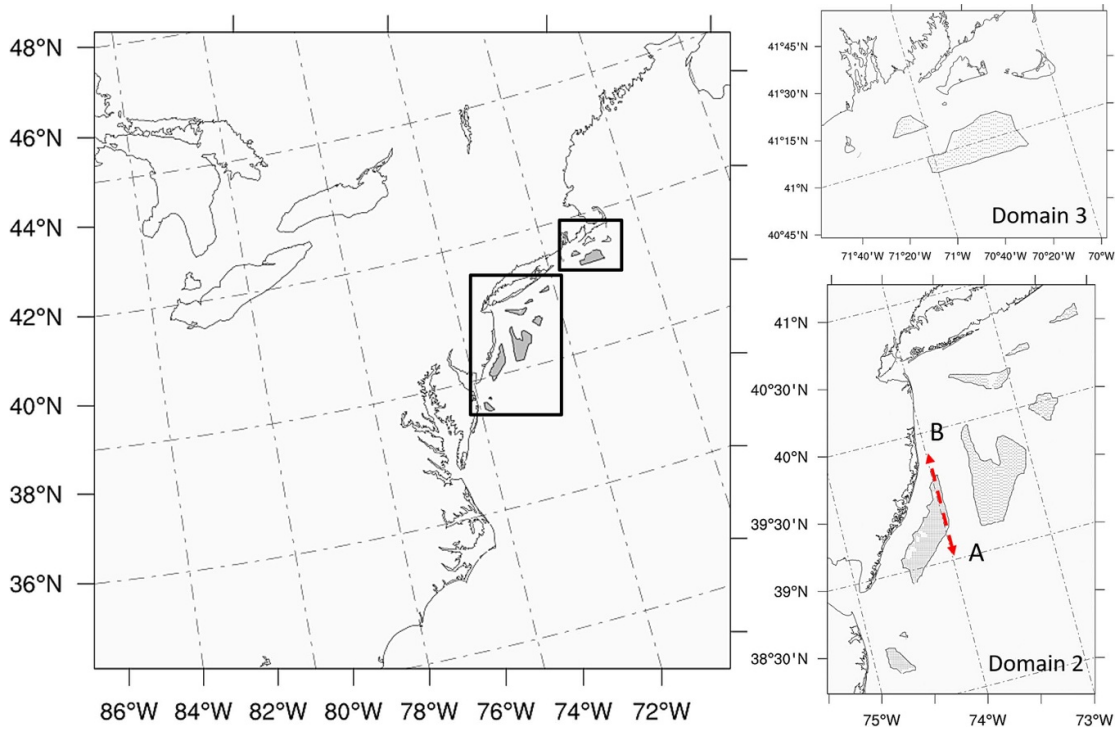

Figure 1. Computational domains: parent domain with 400 × 400 grid cells (4 km resolution), Domain 2 with 260 × 170, and Domain 3 with 105 × 132 (1.33 km resolution for both). The turbine locations are shown with grey dots and the edges of the planned WEAs with grey lines. Results for Domain 3 are presented in the supplementary appendix.

We focus on the offshore WEAs planned along the U.S. East Coast (figures 1). The WEAs are designed and leased by the U.S. Bureau of Ocean Energy Management [11, 44], which is planning for over 30 GW of offshore wind development by 2030 [43]. Details about the location of the leased and planned wind farm locations, as well as their power production, are obtained from [3, 11].

The turbine placement is such that the leased areas are filled prior to the planned areas, as is expected in reality; if the leased areas did not have adequate space to satisfy the power production by the states, then we place the turbines in the planned areas [11, 44]. The turbines are always placed closest to the coast first. The minimum pairwise distance between turbines is 8–10D; as a result, we place at most one turbine per grid cell (more details on the grid are in the next section 2.1).

2.1. Model configuration

We run the WRF model with a two-way nested grid configuration consisting of a parent domain (Domain 1), with a horizontal grid resolution of 4 km and 400 × 400 grid points, containing two separate nested domains, both with a horizontal grid resolution of 1.33 km (figure 1). Domain 2 covers the WEAs from New York to Maryland with 172 × 262 grid points and Domain 3 covers the WEAs from Massachusetts to Rhode Island with 105 × 132 grid points. Here we focus on Domain 2; results from Domain 3 are in the supplementary information(available online at stacks.iop.org/ERL/17/064021/mmedia). In two-way nesting, the model equations are solved first for all the grid cells of the parent domain, which then provides boundary conditions for the sub-domains. The model equations are then solved for all the grid points of the sub-domains. Then, the values obtained at the fine grid cells replace those in the coarse grid cell to ensure that the high-resolution information is not lost but 'fed back' to the coarse domain. The wind farm parameterization is only turned on in the sub-domains.

The North American Mesoscale Forecast System (NAM) model [26] with a horizontal resolution of 12 km provides the initial and boundary conditions for Domain 1. The simulations cover the period from 00:00 UTC on 1 June 2018, to 00:00 UTC on 1 September 2018. The runs are re-initialized every two days with the NAM to avoid potential numerical errors (see section 2.3). Every run starts at 18:00 UTC on the prior day and continues for 54 h. The first 6 h of every simulation are considered as spin-up time and are not included in any later analysis.

To accurately simulate the boundary layer features, special care is devoted to the vertical levels in the WRF runs. Vertical resolution is important to understand wake dynamics and TKE evolution [25], both of which are crucial in this study. The height of the first model level above the ground is especially important, as the heat fluxes are sensitive to this height through the changes to the heat transfer coefficient

Table 1. Details of the WRF model setup.

Parameter	Selection/Value
WRF model version	4.3
Wind farm parameterization	Fitch with TKE advection and default C_{TKE}
Simulation period	1 June—31 August 2018
Extreme-scale wind turbines	DTU-10MW, NREL-15MW
Extreme-scale turbine hub height	119 m, 150 m
Extreme-scale turbine diameter	178 m, 240 m
Conventional wind turbine	Gamesa G128-4.5MW
Conventional turbine hub height	81 m
Conventional turbine diameter	128 m
Initial/boundary conditions	NAM reanalysis, 6 h, 12 km resolution
LSM	Noah-modified 21-category IGBP-MODIS
PBL Scheme	MYNN2
Shortwave radiation	RRTMG shortwave
Longtwave radiation	RRTMG scheme
SST update	NASA-JPL 1 km resolution data

[16]. Several recent studies have further illustrated the need for multiple vertical levels across the rotor [23, 30, 35] and at least 10 m resolution below the rotor [42]. Therefore, we impose 35 vertical levels that are closely-spaced near the surface and then gradually expand. The top hydrostatic pressure is 20 hPa and the lowest model level is at approximately 3.5 m above mean sea level (AMSL). The vertical spacing below 250 m is such that it allows for eight vertical levels within the rotor area, with mass points at approximately 42, 67, 82, 97, 120, 145, 170, and 215 m, and four levels below the rotor area, with mass points at 3.5, 10, 19, and 27 m. Further details about the model setup are provided in table 1.

2.2. Land use and sea surface temperature modifications

The shape and land use of the coastlines influence the meteorology through land-atmosphere interactions at the micro- and meso-scale levels [24, 33]. It is therefore important to have an accurate representation of the coastlines to predict the turbulent heat fluxes and other properties correctly [32], including timing and track of the sea breeze circulation. To this end, we modified the land use in the WRF default input, which is the 21-class moderate resolution imaging spectroradiometer (MODIS) land use database [37]. In the MODIS database, several barrier islands and bays on the coast of New Jersey, Maryland, Long Island, and Delaware, were not defined as land but rather as water. We manually edited the land mask, land use index, and land use fraction fields based on a high-resolution shapefile obtained from NOAA [27] for the coastal areas. As a result of this modification, the model accurately identifies the barrier islands and the bays along the coast.

The sea surface temperature (SST) in the default NAM dataset has a horizontal resolution of 12 km while the distance between the barrier islands and the coast is at most ∼6–7 km. This implies that, with the default SST resolution, the bay temperature is considered the same as the ocean temperature. In addition, every cell of the SST dataset contains about 81 model grid cells. To address this issue, in addition to the improved high-resolution topography, we use 0.01-degree (∼1 km) resolution global daily-varying SST data obtained from NASA JPL [29] to improve the differential heating and the sea/land breeze characteristics.

2.3. Model instabilities

Due to the complex topography of the study domain and the common occurrence of convective systems in summer, the model occasionally created numerical noise that started in a few grid cells over the steep topography or the ocean and grew rapidly and unrealistically over the simulation period. This introduced difficulties in distinguishing between physical phenomena and those created by numerical errors when calculating differential properties (WF—NF). One may interpret the results of numerical noise as physical phenomena and wrongfully attribute them to the wind farms.

To overcome the non-physical numerical noise [4, 30, 52] in the coarse domain, we decreased our simulation periods to a maximum of 54 h based on the recurrence of instabilities and re-initialized the WRF simulations with the NAM fields every other day. In addition, we used four-dimensional grid nudging [41] in the outer domain to damp the higher frequency fluctuations that often cause instabilities. No nudging was applied to the fine domains where the wind farm parameterization is active. The wakes created by the wind farms in the fine domains can travel long distances and can continue into the coarse domain. To minimize the interference of the nudging method with the wind turbine wakes in the coarse domain, we limited the nudging in the coarser domain to levels above 600 m AMSL (i.e. above the 14th model level).

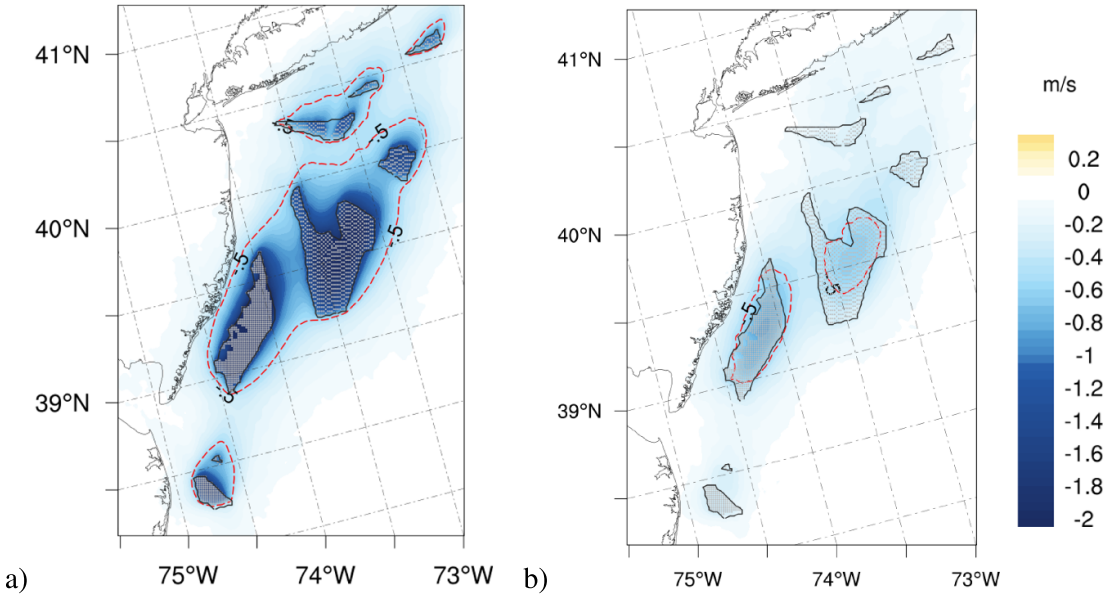

Figure 2. Wind speed changes due to the wind farms (WF–NF) in Domain 2, averaged over 3 summer months: (a) at hub height (∼120 m AMSL) and (b) at the surface. The red-dashed line shows the contour of 0.5 m s^{-1} wind speed deficit, which is considered as the edge of the wake.

3. Results and discussion

In this section, we document how the marine boundary layer responds to extreme-scale wind turbines arranged in large offshore wind farms, such as those proposed for the U.S. East Coast and chosen here as the case study, and analyze the changes caused by them to several meteorological variables. The impact of the offshore wind farms is evaluated by taking the difference between the results of simulations with the farms ('WF', comprising 2252 extreme-scale turbines) minus those of the control case with no farms ('NF'). All the results presented in this section are averaged over a three-month study period in summer 2018.

We find a significant decrease in the local (i.e. at and near the wind farms) average wind speed, up to 2 m s^{-1} (a ∼20% reduction) at hub height (figures 2(a) and S1(a)). The hub-height wind speed deficit is highest within the farms and decreases with downwind distance from the farm in the wakes. An average wind speed deficit of 0.5 m s^{-1}—which is approximately the accuracy of wind speed measurement instruments, like lidars, and which can be used to track the wake edge—extends to about 50 km along the prevailing wind direction, which is south-southwest in the summer [5]. However, on particular days, the wakes from different wind farms merge to form one combined wake that may extend up to approximately 150 km along the wind direction, and anomalous flow acceleration regions form on the sides of the wake (figure S3).

The wakes extend not only in the horizontal, but also vertically. In the vertical, an average wind speed deficit of 0.5 m s^{-1} reaches approximately 350 m AMSL at all wind farms (not shown); it also reaches the surface within the wind farms and in the wakes (figures 2(b) and S1(b)). The wake at the surface causes at most a 0.5 m s^{-1} reduction (∼10% reduction) in average wind speed within the wind farm areas.

Friction velocity (u^*) is directly related to surface stress. Due to the wind turbine wakes, wind speed at the surface decreases, which reduces air-sea friction. Changes in u^* due to the wind farms are in fact negative, meaning that friction velocity is reduced (∼6%) at the surface as a result of the wind farm wakes (figure 3(a)). Similarly, TKE is reduced (∼13%) at the surface over the ocean and parts of the land (figure 3(c)).

On the other hand, TKE above the hub height within the rotor area increases significantly due to turbulence induced by the rotation of the ultra-long blades and to shear production (figure 3(d)).

The moisture content of the surface layer is directly related to the latent heat fluxes. The upward moisture fluxes decrease due to the wind farms, with a maximum reduction of almost 4×10^{-6} kg m^{-2} s^{-1} (a 15% reduction, not shown). As a result, the water vapor mixing ratio decreases at the surface in the wake of the farms, resulting in a slightly dryer surface compared to the control case (figure 3(b)).

Perturbations of mean and turbulent wind speed by the wind farms impact the thermodynamics of the marine boundary layer and alter the turbulent fluxes between the water surface and the atmosphere above it. Positive (upward) heat fluxes correspond to unstable atmospheric conditions, which are common offshore in fall and winter [5]. When the atmosphere is stable, like with a thermal inversion in which warmer air stays above cooler air, the heat fluxes are

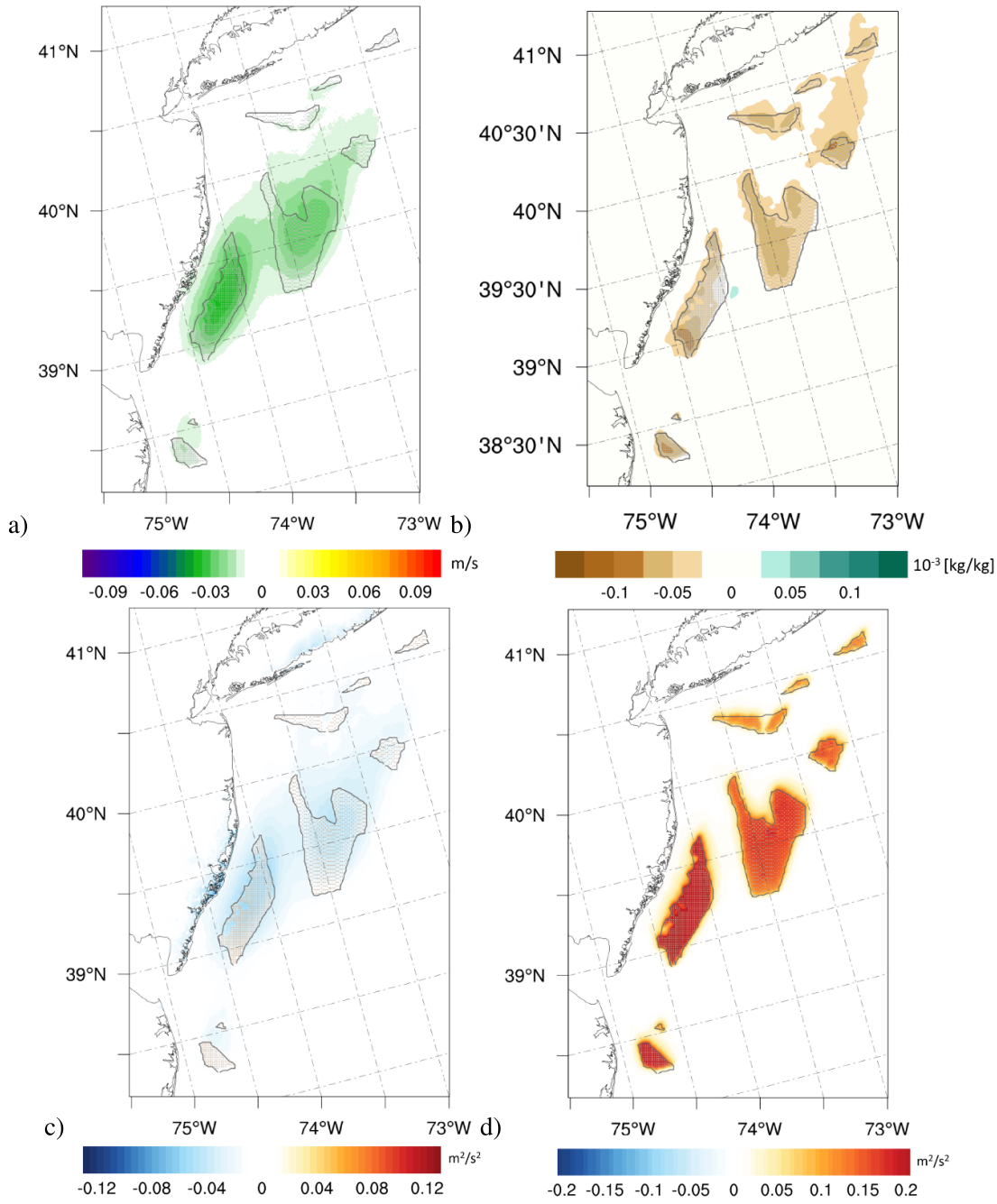

Figure 3. Same as figure 2, but for: (a) friction velocity (u*) at the surface, (b) water vapor mixing ratio at the surface, (c) TKE at the surface, and (d) TKE above hub height (∼200 m AMSL).

downwards; this is the most frequent case offshore in the summer [5]. In this study, stable conditions occurred about 65% of the time and the heat fluxes were negative and downward in general (figure S5).

The temperature changes due to the offshore wind farms differ depending on the height AMSL (figures 4(a)–(c) and S2(a)–(c)). Near the surface, the average temperature changes are minimal and generally limited to the wake areas close to the wind farms (figures 4(c) and S2(c)). These negative temperature changes at the surface (−0.06 K on average) suggest a slight cooling effect by the extreme-scale turbines, in contrast to the generally-accepted warming by conventional turbines in stable conditions [17, 20, 38, 39, 50]. At times, the temperature changes can be stronger, up to −0.8 K (figure S4).

To understand the surface temperature changes, we first note that they are strongly correlated spatially with the heat flux changes at the surface (figures 4(d) and S2(d)). In the presence of the farms, the heat fluxes are always weakened in the same wake regions where cooling is found (e.g. compare figures 4(c) and (d)). The weakening of the heat fluxes is manifest by a positive sign of the change when the atmosphere is stable, because the heat fluxes are downward and negative, and by a negative sign when the

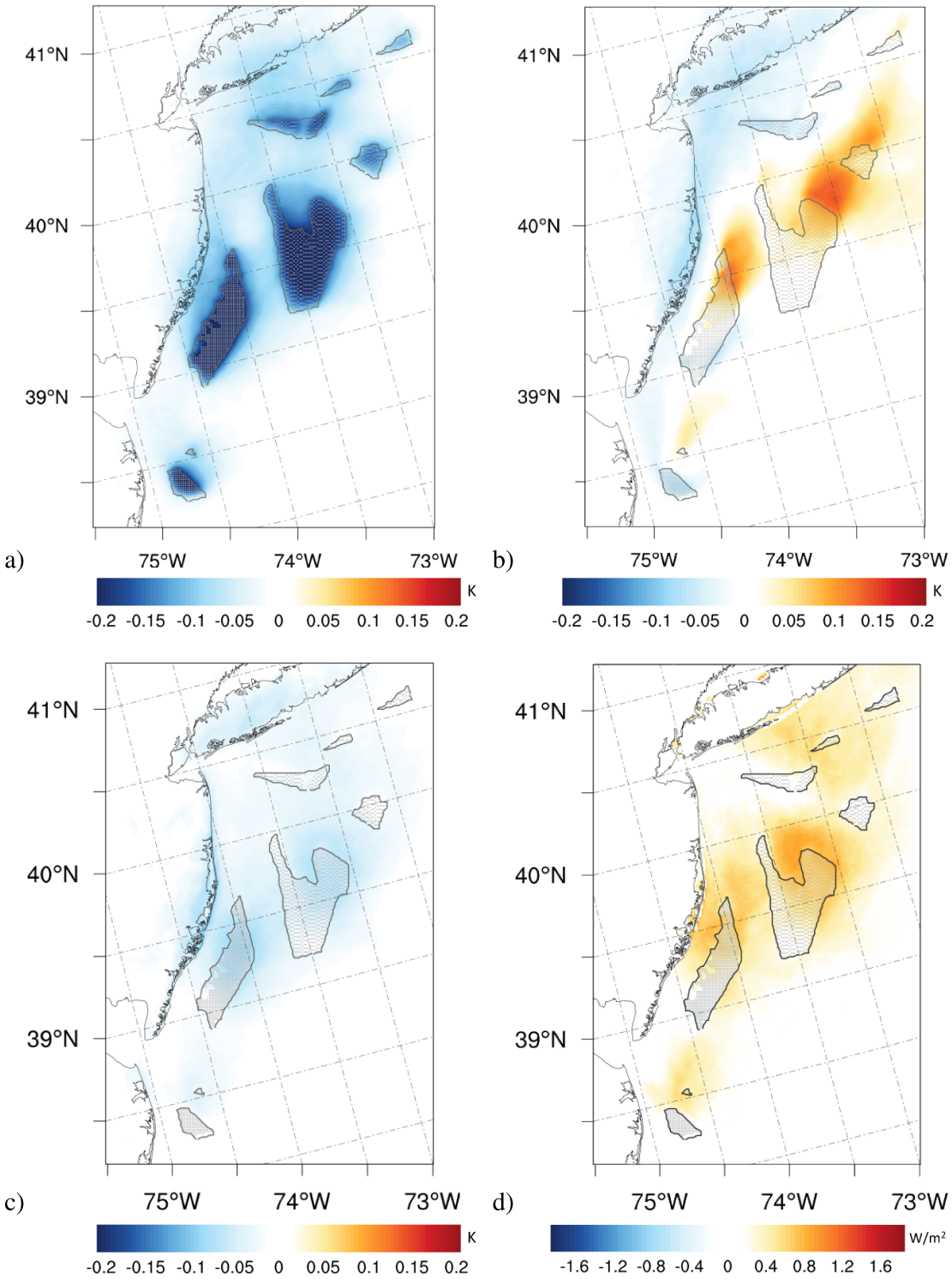

Figure 4. Same as figure 2, but for: (a) temperature above hub height (∼200 m AMSL), (b) temperature below hub height (∼90 m AMSL), (c) temperature at the surface, and (d) sensible heat fluxes at the surface (note that a positive change in downward negative heat flux means a reduction in its magnitude).

atmosphere is unstable, because the heat fluxes are upward and positive. The heat flux reductions are modest (order of 1 W m^{-2} on average), suggesting that less heat is transferred down to the surface and, as a result, slight cooling occurs at the surface. The finding of reduced heat fluxes is consistent with [13], but the finding of cooling in stable conditions is contrary to the majority of the literature, according to which a stable atmosphere is associated with warming at the surface imposed by wind turbines. As such, further examination of the issue is granted. We find that the size, in particular the height, of these ultra-tall offshore wind turbines is the key to understand why they cause different impacts on the atmospheric thermodynamics compared to conventional shorter turbines.

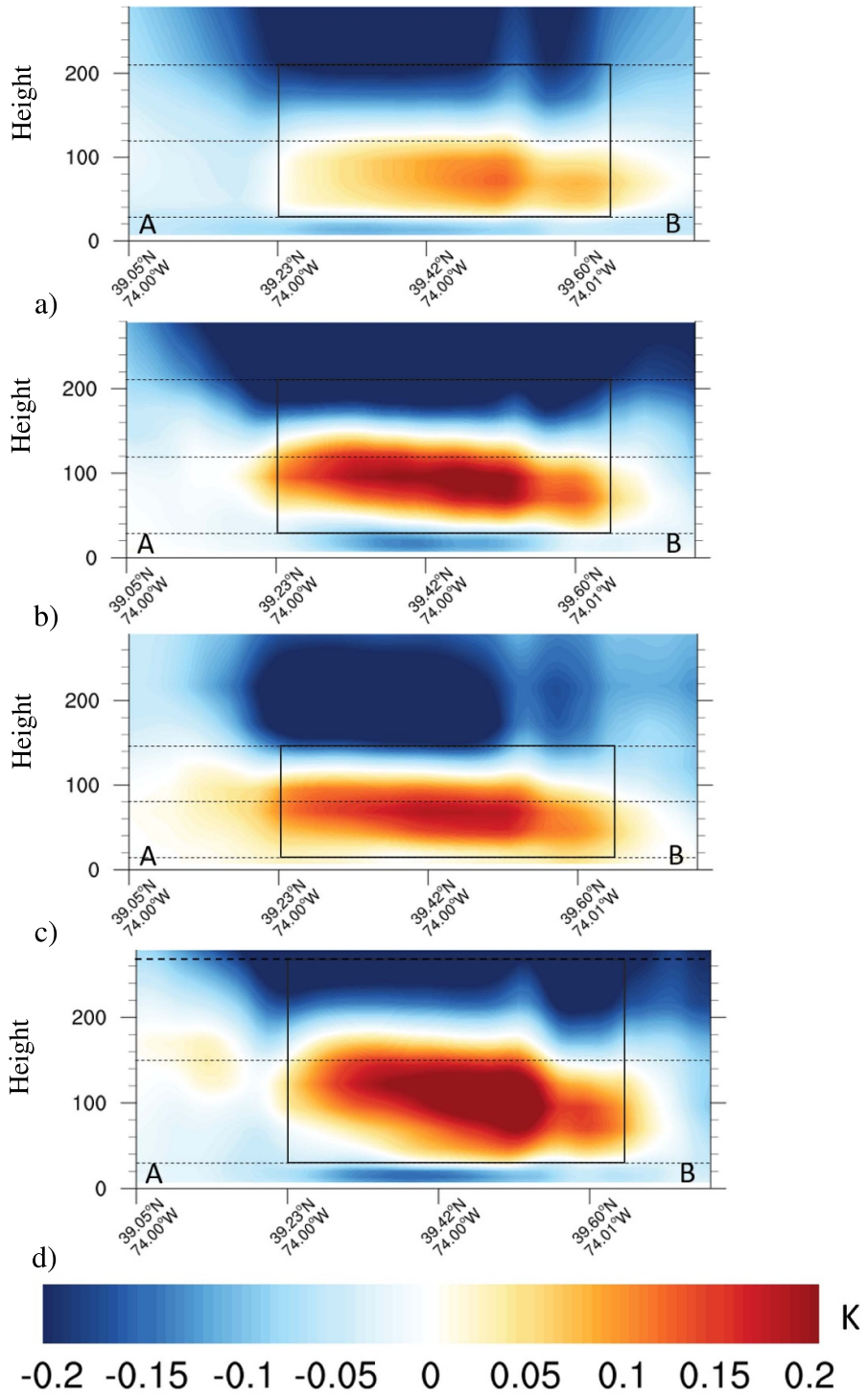

Figure 5. Vertical cross-sections of temperature changes due to the presence of the wind farms (WF–NF) in Domain 2 at points A-B in figure 1: (a) three-month average over summer 2018, (b) one-week average during stable atmospheric conditions with extreme-scale turbines ($H = \sim$120 m), (c) same one-week average as in (b) but with conventional shorter turbines ($H = \sim$80 m), and (d) same one-week average as in (c) but with even taller extreme-scale turbine ($H = \sim$150 m). The box frame indicates the location of the wind farm and the dashed lines indicate the rotor upper tip, hub height, and rotor lower tip.

A recent study [50] proposed that the mechanism that drives changes in near-ground temperature in the presence of turbine wakes is the vertical convergence of turbulent heat fluxes below the rotor. They showed that turbulence and turbulent heat fluxes are enhanced above hub height and reduced (or unchanged) near the ground under all stabilities. During stable conditions, this causes an increase in heat flux convergence under the rotor which, ultimately, results in warming near the ground. Other studies of inland wind farms [17, 47, 51, 53, 54] similarly reported warming at the surface during stable conditions. Our results show an enhancement in vertical mixing above the hub height within the

rotor area (figure 3(d)) and a reduction at the surface (figures 3(a) and (c)), accompanied by cooling above the rotor (figure 4(a)) and warming below it (figure 4(b)), consistent with past studies, but also a slight cooling at the surface in stable conditions (figure 4(c)), inconsistent with past studies.

A hint on this issue comes from the vertical distribution of temperature changes across a wind farm (marked with A-B in figure 1). Consistent with previous literature, the divergence of heat fluxes above the turbines causes cooling above the rotor, mostly limited to the wind farm areas (figures 4(a) and 5(a)). Warming below the rotor still occurs with extreme-scale turbines, due to the convergence of heat fluxes (figures 4(b) and 5(a)). However, with the extreme-scale taller turbines, the warming does not reach the surface, where, instead, the reduction in heat fluxes (figure 4(d)) dominates the temperature response and creates a slight cooling.

To verify that the cooling effects at the surface are indeed due to the turbine height, a week-long simulation of the same WF case but with conventional shorter wind turbines (table 1) confirms that the warming below the rotor due to the heat flux convergence reaches the surface with conventional turbines (figure 5(c)), but remains elevated with the extreme-scale turbines (figure 5(b)).

Preliminary results for the same week but with an even taller extreme-scale wind turbine, the NREL 15 MW turbine [19] with diameter $D = 240$ m and $H = 150$ m (table 1), show a similar magnitude and spatial distribution of temperature changes to those from the DTU-10MW (figure 5(d)), confirming that the results obtained here can be used as a valid benchmark for extreme-size turbines.

The changes in moisture content due to the offshore wind farms also differ depending on the turbine size (figures S6 and S7), with stronger drying caused by conventional shorter turbines (figures S6(a) and S7(a)). In contrast, the taller the turbine is, the weaker the drying becomes, and instead there is a slight increase in moisture content in the wake of the tallest turbines (figures S6(b) and (c) and S7(b) and (c)). The vertical distribution of increase/decrease in moisture content in the presence of the wind farms show a significant correlation with the vertical profile of temperature changes. This suggests that with taller turbines, cooling at the surface dominates the reduction in moisture fluxes and this causes a slight increase in moisture content where the cooling is significant. Overall, the changes to moisture content at the surface are less than 1%.

4. Conclusions

We simulated the potential changes to near-surface atmospheric properties caused by large offshore wind farms equipped with extreme-scale offshore wind turbines using the Advanced Research WRF modeling system and the Fitch wind farm parameterization. As case study, we selected the planned U.S. offshore WEAs, which will total 30 GW by 2030. We conducted high-resolution simulations over the summer of 2018 in the presence and absence of offshore wind farms and studied the differences between the two cases.

Our results show that, at hub height, an average wind speed deficit of 0.5 m s^{-1} extends up to 50 km downwind from the edge of the farms. The wind speed deficit is strongest at the hub height of the wind turbines ($\sim$2 m s^{-1}, or a 22% reduction). The wakes expand in the vertical and create an average wind speed reduction at the surface that is 0.5 m s^{-1} or less (a 10% maximum reduction) within the farms. The wakes also expand in the horizontal, causing a negligible average reduction of near-surface wind speed downstream of the wind farms, order of 3%–4%, but they do not reach the coastline on average. The reduction in wind speed at the surface results in a reduction in surface stress, which reduces friction velocity and TKE at the surface.

Sensible heat fluxes are downward for the majority of the time in the summer, which is an indicator of a stably-stratified atmosphere over the ocean. The downward heat fluxes weaken in the presence of the wind turbine wakes, transferring less heat to the surface from the air. This results in a slight cooling, up to -0.06 K, at the surface in the summer. We find that the surface cooling is specific to the extreme-scale wind turbines. We tested the impacts of conventional (i.e. shorter) wind turbines and found warming at the surface in stable conditions, which is in agreement with the findings in the literature for stable conditions. The warming created below the rotor by the convergence of heat fluxes—previously identified in the literature as the cause of near-surface warming in stable conditions—reaches the surface with conventional wind turbines, but it remains elevated with extreme-scale wind turbines, because they are significantly taller than conventional wind turbines. The warming below the rotor still forms with extreme-scale wind turbines, but it does not reach the surface where, instead, the decrease in the magnitude of sensible heat fluxes dominates and causes a slight cooling. We repeated the simulation with an even taller NREL-15MW wind turbine with hub height at 150 m AMSL and found similar cooling result as with the DTU-10MW turbine.

Moisture and latent heat fluxes also decrease at the surface, with a maximum reduction of approximately 8 W m^{-2} (a 15% reduction) at the wind farms. As a result, water vapor mixing ratio decreases in the wake of the turbines, resulting in a slightly dryer surface compared to the control case. The changes to moisture content also depends on turbine height, with shorter turbines showing a stronger drying signal at the surface at the farms. Overall, the changes to moisture content at the surface are less than 1%.

The results of this study indicate that, on average, meteorological changes at the surface induced by next-generation extreme-scale offshore wind turbines will be nearly imperceptible in the summer. Future research is needed to investigate alternative strategies to calculate the correction factor for TKE source in the parameterization, as well as to explore changes in other seasons and possible effects on air quality.

Data availability statement

The data that support the findings of this study are openly available at the following URL/DOI: https://github.com/golbazimaryam/Golbazi_WRF_input_files.

Acknowledgments

Partial funding for this research came from the University of Delaware (UD) Graduate College Doctoral Fellowship and from the Delaware Natural Resources and Environmental Control (DNREC, Award No. 18A00378), and UD School of Marine Science and Policy graduate fellowship. The simulations were conducted on the UD Caviness, and NCAR Cheyenne high-performance computer clusters.

ORCID iDs

Maryam Golbazi https://orcid.org/0000-0002-5435-7123
Cristina L Archer https://orcid.org/0000-0002-7837-7575

References

[1] Abkar M and Porte-Agel F 2015 A new wind-farm parameterization for large-scale atmospheric models *J. Renew. Sustain. Energy* **7** 013121
[2] Akhtar N, Geyer B, Rockel B, Sommer P S and Schrum C 2021 Accelerating deployment of offshore wind energy alter wind climate and reduce future power generation potentials *Sci. Rep.* **11** 11826
[3] American Wind Energy Association (AWEA) 2020 U.S. offshore wind industry, status update, November 2020 (available at: https://awea.org/offshorewind) (Accessed 1 December 2020)
[4] Ancell B C, Bogusz A, Lauridsen M J and Nauert C J 2018 Seeding chaos: the dire consequences of numerical noise in NWP perturbation experiments *Bull. Am. Meteorol. Soc.* **99** 615–28
[5] Archer C L, Colle B A, Veron D L, Veron F and Sienkiewicz M J 2016 On the predominance of unstable atmospheric conditions in the marine boundary layer offshore of the U.S. northeastern coast *J. Geophys. Res.: Atmos.* **121** 8869–85
[6] Archer C L, Vasel-Be-Hagh A, Yan C, Wu S, Pan Y, Brodie J F and Maguire A E 2018 Review and evaluation of wake loss models for wind energy applications *Appl. Energy* **226** 1187–207
[7] Archer C L, Wu S, Vasel-Be-Hagh A, Brodie J F, Delgado R, St A Oncley P, S and Semmer S 2019 The VERTEX field campaign: observations of near-ground effects of wind turbine wakes *J. Turbul.* **20** 64–92
[8] Archer C L, Wu S, Ma Y and Jiménez P A 2020 Two corrections for turbulent kinetic energy generated by wind farms in the WRF model *Mon. Weather Rev.* **148** 4823–35
[9] Baidya Roy S 2004 Can large wind farms affect local meteorology? *J. Geophys. Res.: Atmos.* **109** D19
[10] Bak C, Zahle F, Bitsche R, Kim T, Yde A, Henriksen L C, Hansen M H, Blasques J P A A, Gaunaa M and Natarajan A 2013 The DTU 10-MW reference wind turbine *Danish Wind Power Research 2013*
[11] Bennet J and Feinberg F 2018 Outer continental shelf wind energy; leasing in the New York Bight (available at: www.boem.gov/sites/default/files/renewable-energy-program/State-Activities/NY/Bennett-and-Feinberg-presentation.pdf) (Accessed 1 March 2022)
[12] Blahak U, Goretzki B and Meis J 2010 A simple parameterization of drag forces induced by large wind farms for numerical weather prediction models *Proc. European Wind Conf. and Exhibition*
[13] Boettcher M, Hoffmann P, Lenhart H-J, Schlünzen H and Schoetter R 2015 Influence of large offshore wind farms on North German climate *Meteorol. Z.* **24** 465–80
[14] Christiansen M B and Hasager C B 2005 Wake effects of large offshore wind farms identified from satellite SAR *Remote Sens. Environ.* **98** 251–68
[15] Fitch A C 2016 Notes on using the mesoscale wind farm parameterization of Fitch *et al* (2012) in WRF *Wind Energy* **19** 1757–8
[16] Fitch A C, Olson J B and Lundquist J K 2013 Parameterization of wind farms in climate models *J. Clim.* **26** 6439–58
[17] Fitch A C, Olson J B, Lundquist J K, Dudhia J, Gupta A K, Michalakes J and Barstad I 2012 Local and mesoscale impacts of wind farms as parameterized in a mesoscale NWP model *Mon. Weather Rev.* **140** 3017–38
[18] Foreman R J, Cañadillas B, Neumann T and Emeis S 2017 Measurements of heat and humidity fluxes in the wake of offshore wind turbines *J. Renew. Sustain. Energy* **9** 053304
[19] Gaertner E *et al* 2020 IEA wind TCP task 37: definition of the IEA 15-megawatt offshore reference wind turbine *Technical Report* (Golden, CO: National Renewable Energy Lab (NREL))
[20] Harris R A, Zhou L and Xia G 2014 Satellite observations of wind farm impacts on nocturnal land surface temperature in Iowa *Remote Sens.* **6** 12234–46
[21] Hasager C, Vincent P, Badger J, Badger M, Di Bella A, Peña A, Husson R and Volker P 2015 Using satellite SAR to characterize the wind flow around offshore wind farms *Energies* **8** 5413–39
[22] Jacobson M Z 2005 *Fundamentals of Atmospheric Modeling* 2nd edn (Cambridge: Cambridge University Press)
[23] Lee J C Y and Lundquist J K 2017 Evaluation of the wind farm parameterization in the weather research and forecasting model (version 3.8.1) with meteorological and turbine power data *Geosci. Model Dev.* **10** 4229–44
[24] Li X, Mitra C, Dong L and Yang Q 2018 Understanding land use change impacts on microclimate using weather research and forecasting (WRF) model *Phys. Chem. Earth* A B C **103** 115–26
[25] Mangara R, Guo Z and Li S 2019 Performance of the wind farm parameterization scheme coupled with the weather research and forecasting model under multiple resolution regimes for simulating an onshore wind farm *Adv. Atmos. Sci.* **36** 119–32
[26] National Oceanic and Atmosphere Administration (NOAA) North American mesoscale forecast system; NAM analyses (available at: www.ncei.noaa.gov/data/north-american-mesoscale-model/access/analysis/) (Accessed 1 March 2022)
[27] National Oceanic and Atmospheric Administration (NOAA) 2016 NOAA medium resolution shoreline (available at: https://shoreline.noaa.gov/data/datasheets/medres.html) (Accessed 15 December 2021)

[28] Pan Y and Archer C L 2018 A hybrid wind-farm parametrization for mesoscale and climate models *Bound.-Layer Meteorol.* **168** 469–95
[29] Physical Oceanography Distributed Active Archive Center; JPL MUR MEaSUREs Project 2015 GHRSST level 4 MUR global foundation sea surface temperature analysis (v4.1) version 4.1 (available at: https://podaac.jpl.nasa.gov/dataset/MUR-JPL-L4-GLOB-v4.1) (Accessed 8 February 2022)
[30] Pryor S C, Shepherd T J, Volker P J H, Hahmann A N and Barthelmie R J 2020 "Wind Theft" from onshore wind turbine arrays: sensitivity to wind farm parameterization and resolution *J. Appl. Meteorol. Climatol.* **59** 153–74
[31] Rajewski D A *et al* 2013 Crop wind energy experiment (CWEX): observations of surface-layer, boundary layer and mesoscale interactions with a wind farm *Bull. Am. Meteorol. Soc.* **94** 655–72
[32] Román-Cascón C, Lothon M, Lohou F, Hartogensis O, de Arellano J V-G, Pino D, Yagüe C and Pardyjak E R 2021 Surface representation impacts on turbulent heat fluxes in the weather research and forecasting (WRF) model (v.4.1.3) *Geosci. Model Dev.* **14** 3939–67
[33] Schicker I, Arias D A and Seibert P 2016 Influences of updated land-use datasets on WRF simulations for two Austrian regions *Meteorol. Atmos. Phys.* **128** 279–301
[34] Siedersleben S K *et al* 2018 Evaluation of a wind farm parametrization for mesoscale atmospheric flow models with aircraft measurements *Meteorol. Z.* **27** 401–15
[35] Siedersleben S K *et al* 2020 Turbulent kinetic energy over large offshore wind farms observed and simulated by the mesoscale model WRF (3.8.1) *Geosci. Model Dev.* **13** 249–68
[36] Skamarock W C, Klemp J B, Dudhia J, Gill D O, Barker D M, Wang W and Powers J G 2005 A description of the advanced research WRF version 2 *Technical Report* NCAR/TN-468+STR (National Center for Atmospheric Research)
[37] Skamarock W C *et al* 2019 A description of the advanced research WRF model version 4 *Technical Report* NCAR/TN-556+STR (National Center for Atmospheric Research)
[38] Slawsky L M, Zhou L, Roy S B, Xia G, Vuille M and Harris R A 2015 Observed thermal impacts of wind farms over Northern Illinois *Sensors* **15** 14981–5005
[39] Smith C M, Barthelmie R and Pryor S 2013 *In situ* observations of the influence of a large onshore wind farm on near-surface temperature, turbulence intensity and wind speed profiles *Environ. Res. Lett.* **8** 034006
[40] Spellman F R 2016 *The Science of Air: Concepts and Applications* (Boca Raton, FL: CRC Press)
[41] Stauffer D R and Seaman N L 1994 Multiscale four-dimensional data assimilation *J. Appl. Meteorol. Climatol.* **33** 416–34
[42] Tomaszewski J M and Lundquist J K 2020 Simulated wind farm wake sensitivity to configuration choices in the weather research and forecasting model version 3.8.1 *Geosci. Model Dev.* **13** 2645–62
[43] US Department of Interior (DOI) 2021 Secretary Haaland outlines ambitious offshore wind leasing strategy (available at: www.doi.gov/pressreleases/secretary-haaland-outlines-ambitious-offshore-wind-leasing-strategy) (Accessed 31 January 2022)
[44] US Deparment of Interior; Bureau of Ocean Energy management (BOEM) Renewable energy GIS data (available at: www.boem.gov/renewable-energy/mapping-and-data/renewable-energy-gis-data) (Accessed 1 March 2022)
[45] Vermeer L, Sørensen J N and Crespo A 2003 Wind turbine wake aerodynamics *Prog. Aerosp. Sci.* **39** 467–510
[46] Volker P J, Badger J, Hahmann A N and Ott S 2015 The explicit wake parametrisation V1.0: a wind farm parametrisation in the mesoscale model WRF *Geosci. Model Dev.* **8** 3715–31
[47] Walsh-Thomas J M, Cervone G, Agouris P and Manca G 2012 Further evidence of impacts of large-scale wind farms on land surface temperature *Renew. Sustain. Energy Rev.* **16** 6432–7
[48] Wang Q, Luo K, Wu C and Fan J 2019 Impact of substantial wind farms on the local and regional atmospheric boundary layer: case study of zhangbei wind power base in China *Energy* **183** 1136–49
[49] Wang Q, Luo K, Wu C, Zhu Z and Fan J 2022 Mesoscale simulations of a real onshore wind power base in complex terrain: wind farm wake behavior and power production *Energy* **241** 122873
[50] Wu S and Archer C L 2021 Near-ground effects of wind turbines: observations and physical mechanisms *Mon. Weather Rev.* **149** 879–98
[51] Xia G, Zhou L, Freedman J M, Roy S B, Harris R A and Cervarich M C 2016 A case study of effects of atmospheric boundary layer turbulence, wind speed and stability on wind farm induced temperature changes using observations from a field campaign *Clim. Dyn.* **46** 2179–96
[52] Zhang F, Snyder C and Rotunno R 2003 Effects of moist convection on mesoscale predictability *J. Atmos. Sci.* **60** 1173–85
[53] Zhou L, Tian Y, Roy S B, Dai Y and Chen H 2013 Diurnal and seasonal variations of wind farm impacts on land surface temperature over western Texas *Clim. Dyn.* **41** 307–26
[54] Zhou L, Tian Y, Roy S B, Thorncroft C, Bosart L F and Hu Y 2012 Impacts of wind farms on land surface temperature *Nat. Clim. Change* **2** 539